Available online at www.sciencedirect.com
ScienceDirect
International Journal of Mechanical Sciences 49 (2007) 589–596
International Journal of Mechanical Sciences
www.elsevier.com/locate/ijmecsci

Analytical remarks on the anchorage of elastic–plastically bonded ductile bars

Maurizio Froli*

Department of Structural Engineering, University of Pisa, Via Diotisalvi, 2 I-56126 Pisa, Italy

Received 4 September 2006; accepted 27 September 2006
Available online 21 November 2006

Abstract

A simple analytical extension of Hermite–Bresson's results to the domain of the irreversible relative displacements allows the description of the non-linear force–displacement response of a tensile bar embedded in a massive support by means of an elastic–plastic bonding agent.

The analytical model evidences the influence of the main governing parameters on the attainment of two ideal anchorage conditions of plasticity initiation occurring in the bar simultaneously with that of the bond material (anchorage length L_{IP}), or of plasticity initiation occurring in the bar just after the complete yielding of this one (anchorage length L_{CP}).

The ratio between the expressions of these two anchorage lengths reveals an interesting, compact mathematical form of eloquent mechanical meaning which allows the immediate determination of anchorage length L_{IP}.

Keywords: Anchorage; Anchorage length; Bond; Bond failure; Slip; Elasto-plasticity

1. Introduction

Bond action between heterogeneous materials is at the basis of every composite structural behaviour, indifferently if exerted by chemical adhesion of some gluing substance or by mechanical indentation of the contact surfaces.

Its importance justifies the enormous amount of research activity that has been dedicated to this topic until now. Among all application fields, reinforced concrete seems to be typically that one where bond problems have been most widely and deeply investigated both under the aspect of the traditional coupling of ribbed bars with cast-in-place concrete masses or under the aspect of more recent strengthening techniques where metallic or synthetic bars are glued in drilled holes or grooves within already hardened concrete supports [1], and metallic plates are fixed on concrete surfaces by means of adhesive materials [2].

Numberless experimental researches have evidenced extremely many different aspects of this complex mechanical action and generations of theoreticians have devoted their investigations to the effort of developing always more and more refined analytical and numerical models[1] in order to better describe and predict the most part of all these experimental evidences.

Calculations of steel-to-concrete bond stress distributions were for example already performed by Losberg [7] and Tepfers [8] who wrote in differential form the equation previously introduced in finite terms by Bleich [9] to study the distribution of shear forces in large riveted splices. This direct analytical method, sometimes called *K*-value theory, was also used by L'Hermite and Bresson [2] to model the gluing of steel lamina in the reinforcing of concrete beams. It is based on the hypothesis that bond stresses are directly proportional to the relative displacement between steel and concrete and, in spite of its simplicity, it reveals good in

[1]To have an idea of the quantity of experimental and theoretical contributions produced on this topic, and to realize that it is almost impossible even trying to cite just a concise selection of the most important papers, it is sufficient to give a look at the bibliographies contained in the state-of-the-art reports which have been periodically published by CEB [3,4], ACI Committee 408 [5] and more recently by FIB [6].

*Tel.: +39 5 835706; fax: +30 5 554597.
E-mail address: m.froli@ing.unipi.it.

0020-7403/$ - see front matter © 2006 Elsevier Ltd. All rights reserved.
doi:10.1016/j.ijmecsci.2006.09.016

Nomenclature

A_1 cross section area of the metallic bar (cm^2)
A_2 cross section area of the support material (cm^2)
E_1 Young's modulus of the metallic bar (daN/cm^2)
E_2 Young's modulus of the support material (daN/cm^2)
F_{IP} ratio between the yielding stress in the metallic bar and the yielding stress in the bond springs requested to have contemporary plasticity initiation in both materials
F_{CP} ratio between the yielding stress in the metallic bar and the yielding stress in the bond springs requested to have plasticity initiation in the bar and complete plasticity in the bond springs
k stiffness of the bond springs per unit bond surface and unit slip (daN/cm^3)
$K = k\Sigma$ stiffness of the bond springs per unit length and unit slip (daN/cm^2)
K_{eq} equivalent global stiffness of the entire anchor in the elastic range (N/cm)
L anchorage length (cm)
L_{IP} anchorage length corresponding to the yielding initiation in the bond springs (cm)
L_{CP} anchorage length corresponding to the complete yielding of the bond springs (cm)
P applied tensile force (daN)
P'_y applied tensile force corresponding to the plasticity initiation in the bond springs (daN)
P''_y applied tensile force corresponding to the plasticity initiation in the metallic bar (daN)
P'''_y applied tensile force corresponding to the complete plasticity of the bond springs (daN)
$\underline{t} = \Sigma\tau$ bond forces per unit length of the bar (daN/cm)
$t_y = \Sigma\tau_y$ yielding bond forces per unit length of the bar (daN/cm)
$\Delta\hat{W}_0$ slip between metallic bar and embedding material at the origin of the anchorage length (cm)
$W_1(z)$ elastic displacement in the metallic bar (cm)
$W_2(z)$ elastic displacement in the embedding material (cm)
$\hat{W}_1(z) = \Delta\hat{W}_0 + W_1(z)$ total displacement in the metallic bar (cm)
$\hat{W}_2(z) = W_2(z)$ total displacement in the embedding material (cm)
$\hat{W}'_{1E}$ total displacement at the outer edge of the metallic bar (cm)
$\hat{W}'_{1I}$ total displacement in the metallic bar at the elastic–plastic interface of the bond springs (cm)
z'_y elastic bond length for $P'_y = P = P''_y$
z''_y elastic bond length for $P = P''_y$
α $k\Sigma(1 + E_1A_1/E_2A_2)/E_1A_1$ (cm^{-2})
λ E_1A_1/E_2A_2
σ_{1y} yielding stress of the metallic bar (daN/cm^2)
Σ adherent perimeter of the metallic bar (cm)
τ bond stress (daN/cm^2)
$\tau_c = P/\Sigma L$ mean uniform bond stress (daN/cm^2)
τ_y yielding bond stress (daN/cm^2)

agreement with mesoscopic experimental results (model of macroscopically uncracked concrete).

After these first applications, the differential equation of bond has been of course extended and refined by the introduction of various local non-linear bond–slip relations and also by allowing in the attainment of the inelastic range by the steel.

The integration has been conveniently performed each time with numerical techniques in a number of different approaches (see for example, Refs. [10–13]).

2. Research significance

The highly detailed and realistic amount of information that modern discrete modelling techniques are able to achieve in the local microscopic response of steel bars, differently embedded in a massive medium, requires normally a big amount of computational resources. Sometimes their implementation in large scale calculation schemes of extended systems reveals to be too burdensome if we consider that refined results frequently exceed the needs of structural analysis at macroscopic levels.

On the contrary, current analysis of semi-rigid joints requires simple calculation schemes where the splicing components are modeled by assemblages of springs with suitable force–displacement constitutive law [14]. Similarly, r.c. bars in composite semi-rigid joints, may be effectively modelled by equivalent springs with adequate non-linear force–displacement laws that cumulatively include bond effects.

Moreover, in spite of so many available refined theoretical models, FIB Bulletin [6] still defines L as anchorage length if it is *sufficient to let the bar material yields before the bond layer fails* making no difference weather the bond failure must be reached just locally, can be extended over a finite portion of L or even all over L.

At the same time, also many authors very often consider as bond ultimate state only that corresponding to the complete plasticity of the bond layer (with a uniform distribution of bond stresses) without taking into account intermediate elastic–plastic stages and if the plasticity of the anchor initiates just when the bond material starts yielding or when it is already completely yielded.

The goal of getting a simple and handy analytical description of these progressive failures has been pursued in the present paper. It is based on the well-known Hermite–Bresson differential equation of bond in the elastic range applied to the classic problem of a tensile bar embedded on a finite length in a massive and rather rigid support. The ideal hypotheses are that the connection is developed through a elastic–plastic slip layer where all the properties contributing to the bond action are lumped together.

The simplicity of the model permits a clear and practical parametric and geometric representation of the results and also to evidence, as a secondary consequence, some analytical properties of mechanical interest.

3. Bond modelling in the elastic domain: the Hermite–Bresson equation

Let us consider the problem of coupling together two straight coaxial bars: the first one is fixed at one extreme and the second one is loaded at the edge E by a gradually increasing force P (Fig. 1).

Along the splice length L the bar may be regarded as composed by an inner prismatic core (bar 1) and a coaxial, uniformly thick support of different material (bar 2). The two component parts of the bar are uniformly connected to each other by means of an extremely thin bond medium schematized by a uniform distribution of longitudinal tangential springs.

Let us suppose that the cross sections of the inner and of the outer bar remain plain along L and that relative longitudinal displacements between the two materials are restrained all over the bond length by the springs which react with bond shear stresses τ uniformly distributed, at each section, along the perimeter Σ of the interface.

Under these assumptions the resultants of the tension stresses in both bars, as well as the resultant of the shear forces per unit length: $t = \Sigma\tau$, are ideally applied to the axis of the composite bar and the whole problem is therefore reduced to just one dimension.

The two bars are assumed to be elastic-perfectly plastic with different Young's moduli and yielding points and also the bond springs are supposed to have an elastic-perfectly plastic constitutive law with $t_y = \Sigma\tau_y$ as yielding point (Fig. 2).

Let us put the origin O of the z-axis at the point of bar 2 corresponding to the unloaded end of bar 1 (Fig. 1). If $\Delta\hat{W}_0$ is the slip between the two bars at point O and $W_1(z)$, $W_2(z)$ are, respectively, the axial elastic displacements of the two bars at any point of the anchorage segment L, than the total displacement $\hat{W}_1$ of a generic point of bar 1 with respect to point O is $\hat{W}_1(z) = \Delta\hat{W}_0 + W_1(z)$ while of course $\hat{W}_2(z)$ coincides with $W_2(z)$ (Fig. 3).

The unknown function of the problem is the difference $\Delta\hat{W}(z)$ between the total longitudinal displacement $\hat{W}_1(z)$ of bar 1 and the total longitudinal displacement $\hat{W}_2(z)$ of bar 2, described by the already mentioned equation of bond:

$$\frac{d^2\Delta\hat{W}(z)}{dz^2} - \frac{\kappa\Sigma}{E_1A_1}\left(1 + \frac{E_1A_1}{E_2A_2}\right)\Delta\hat{W}(z) = 0, \quad (1)$$

where A_1 and A_2 are respectively the cross section areas of bar 1 and 2; E_1 and E_2 are, respectively the Young's modulus of bar 1 and 2.

Put

$$\alpha = \sqrt{\frac{\kappa\Sigma}{E_1A_1}\left(1 + \frac{E_1A_1}{E_2A_2}\right)}$$

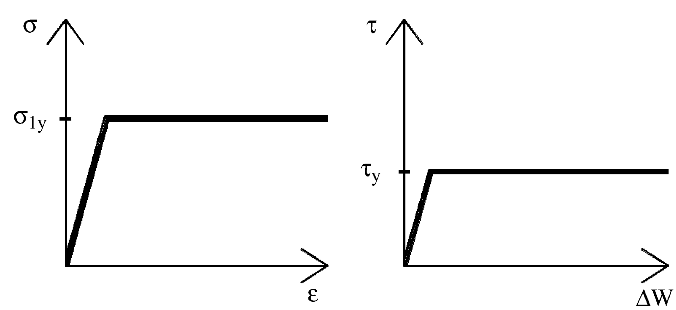

Fig. 2. Constitutive laws of the bar's material and of the bond.

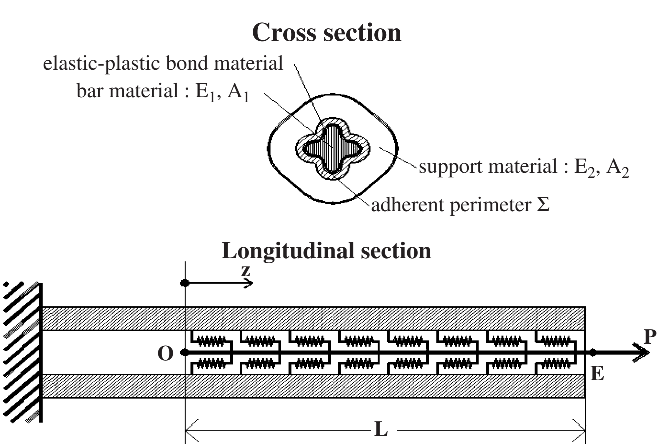

Fig. 1. Scheme of the mechanical model.

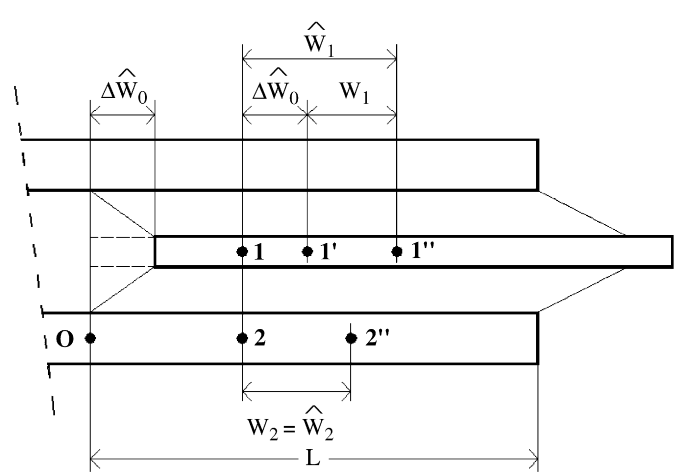

Fig. 3. Notation of the absolute and relative displacements.

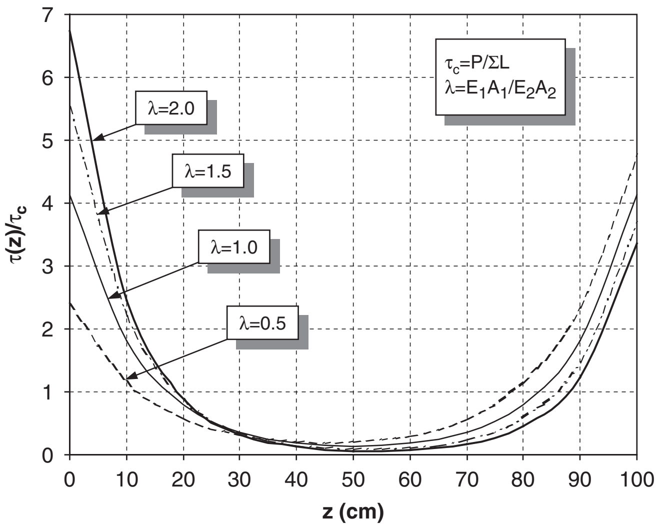

Fig. 4. Shear stress distribution along anchorage length L for different values of λ.

and once integrated Eq. (1), shear stresses along L directly follow as

$$\tau(z) = \kappa \Delta \hat{W}(z) = \frac{P\kappa}{\alpha}\left[\frac{1}{E_1A_1}\frac{\cosh \alpha z}{\sinh \alpha L} + \frac{1}{E_2A_2}\frac{\cosh \alpha(z-L)}{\sinh \alpha L}\right] \tag{2}$$

and are plotted in Fig. 4 for different values of the ratio $\lambda = E_1A_1/E_2A_2$:

4. Elastic–plastic bar embedded in a very rigid support

4.1. Elastic phase

If bar 2 is much stiffer than bar 1, than we can put $E_2A_2 \cong \infty$ into formula (2) and bar 2 can be from this point assimilated to a rigid half space where bar 1 is embedded.

Factor α reduces than to

$$\alpha = \sqrt{\frac{\kappa\Sigma}{E_1A_1}} = \sqrt{\frac{\mathrm{K}}{E_1A_1}} \tag{3}$$

and the equations of the total slip and of the bond stresses assume the reduced forms

$$\Delta\hat{W}(z) = W_1(z) = \frac{P}{\alpha E_1A_1}\frac{\cosh \alpha z}{\sinh \alpha L}, \quad \tau(z) = \frac{P\kappa}{\alpha E_1 A_1}\frac{\cosh \alpha z}{\sinh \alpha L}. \tag{4}$$

The absolute displacements of the unloaded and of the loaded end are given, respectively, by

$$\hat{W}_1(z=0) = \frac{P}{\alpha E_1A_1}\frac{1}{\sinh \alpha L}, \quad \hat{W}_1(z=L) = \frac{P}{\alpha E_1A_1}\frac{1}{\tanh \alpha L} = K_{eq}P. \tag{5}$$

4.2. Phase of plasticity initiation in the bond material

Let us assume now that the bond material yields first, followed by the bar. The yielding process of the bond springs initiates at the loaded edge E of the bar where slip and shear stresses are maximum and propagates towards the other extremity O as qualitatively illustrated in Fig. 5.

The value P'_y of the force P corresponding to the plasticity initiation of the springs is deduced from the condition that

$$\tau_{(z=L)} = \tau_y = \frac{\kappa P'_y}{\alpha E_1 A_1 \tanh(\alpha L)} = \frac{\kappa P'_y}{\sqrt{\mathrm{K}E_1A_1}\tanh(\alpha L)},$$
$$\Rightarrow P'_y = \frac{\tau_y}{\kappa}\sqrt{\mathrm{K}E_1A_1}\tanh(\alpha L) = \frac{t_y}{\alpha}\tanh(\alpha L) \tag{6}$$

and the related displacement $\hat{W}'_{1E}$ is of course equal to $\hat{W}'_{1E} = \mathrm{K}_{eq}P'_y$.

We want now to determine the relation $P = P(\hat{W}'_{1E})$ when $P = P'_y$.

The interface between still elastic and yielded springs is situated in a point I at the distance z'_y from the origin O (Fig. 5).

To calculate z'_y it is sufficient to impose from Eq. (6) that

$$P = t_y\left[\frac{\tanh(\alpha z'_y)}{\alpha} + (L - z'_y)\right]. \tag{7}$$

For each $P > P'_y$ the precedent gives the corresponding distance z'_y of point I.

The displacement of point E is the sum of the elastic elongation of the portion $L - z'_y$ of the bar with the displacement of point I.

In I the tensile force in the bar is

$$N_I = P - t_y\left(L - z'_y\right). \tag{8}$$

Therefore the displacement $\hat{W}_{1I}$ is, according to the second of Eq. (5)

$$\hat{W}_{1I} = \frac{\left[P - t_y(L - z'_y)\right]}{\tanh(\alpha z'_y)\sqrt{\mathrm{K}E_1A_1}} = W_y = \frac{t_y}{\mathrm{K}} = \frac{\tau_y}{k}. \tag{9}$$

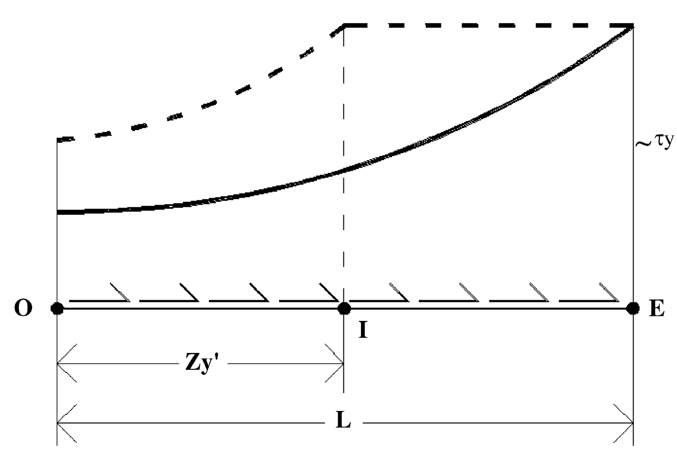

Fig. 5. Qualitative distribution of bond stresses at and after the plasticity initiation of the springs.

On the other hand, the elongation of the portion $(L - z'_y)$ is given by

$$\delta \hat{W}_1 = \int_0^{(L-z'_y)} \frac{N(\bar{z}')}{E_1 A_1} \, \mathrm{d}\bar{z}' = \frac{1}{E_1 A_1} \left[P(L - z'_y) - \frac{t_y}{2}(L - z'_y)^2 \right] \quad (10)$$

and hence

$$\hat{W}_{1E} = \hat{W}_{1I} + \delta \hat{W}_1 = \frac{\left[P - t_y(L - z'_y)\right]}{\tanh(\alpha z'_y)\sqrt{\mathrm{K} E_1 A_1}} + \frac{1}{E_1 A_1}\left[P - \frac{t_y}{2}(L - z'_y)\right](L - z'_y). \quad (11)$$

Correlated couples of values $(P > P'_y, P'_z)$ substituted into the precedent Eq. (11), give the desired relation $P = P(\hat{W}_{1E})$ between the applied force P and the displacement $\hat{W}_{1E}$ of the free edge E of the bar after the yielding of the bond springs is occurred but the bar is still thoroughly elastic.

Fig. 6 contains some force vs. free edge displacement curves for different values of the parameter α, where $L = \text{const.} \; = 100\,\text{cm}$. Non-linear parts of the graphs correspond to the progressive yielding of the springs.

5. Ultimate limit states

As previously said, FIB Bulletin 10 defines anchorage length L that *sufficient to let the bar material yields before the bond layer fails*.

With the help of the present schematization it can be evidenced that two limit situations may be defined in correspondence of the yielding initiation of the bar:

- a limit state of incipient plasticity, when yielding contemporary initiates in the bar and in the bond layer at the outer edge E of the anchorage. Let us denote with L_{IP} the anchorage length that satisfies this condition,

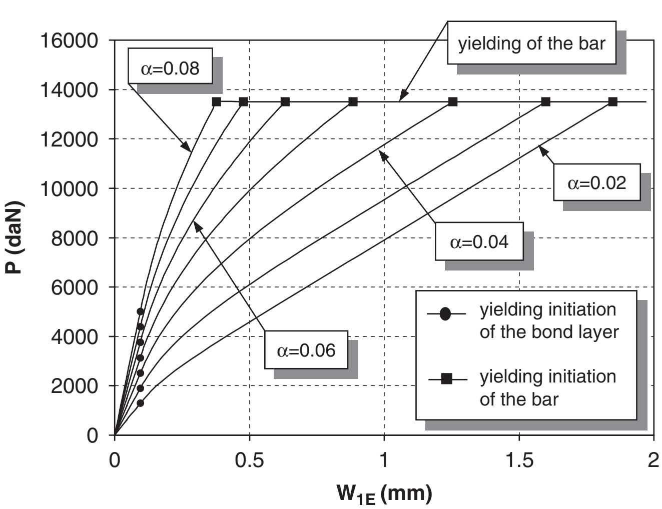

Fig. 6. Force versus free edge displacement relationships at varying α.

- a limit state of complete plasticity, when the yielding of the bar initiates just when the plasticity has spread in the bond layer all over L. Let us denote with L_{CP} the anchorage length that satisfies this condition,

Intermediate states may also take place if the yielding of the bar initiates when the plasticity of the bond layer is not yet complete.

5.1. Limit state of incipient plasticity: L_{IP} anchorage length

The anchored bar initiates to yield from the outer edge E as soon as $\sigma_1 = \sigma_{1y}$.

The corresponding applied force is therefore equal to $P''_y = \sigma_{1y} A_1$ and the distance z''_y from O of the interface I between elastic and plastic bond must satisfy Eq. (7) where P must be put equal to P''_y.

The associated displacement $\hat{W}_{1E}$ is finally obtained by substituting the couple of values P''_y, z''_y into Eq. (11).

From this point on, further displacements of the free edge are assumed to occur at a constant applied force P''_y (see Fig. 6).

Let us state the condition that

$$P'_y = P''_y \quad (12)$$

or that the yielding of the bond material and of the anchored bar initiate contemporary:

$$P'_y = P''_y \Rightarrow \left(\frac{\sigma_{1y}}{\tau_y}\right) = F_{IP} = \frac{\alpha E_1}{\kappa} \tanh(\alpha L). \quad (13)$$

Let us introduce the following quantities which have both the dimension of a length:

$$\frac{E_1}{\kappa} = \psi, \quad \frac{A_1}{\Sigma} = \rho, \quad (14)$$

ψ represents a measure of the ratio between the stiffnesses of the core material and of the bond layer while ρ gives an idea of the extension of the adherent perimeter in comparison with the area of the core cross section. Large values of ρ correspond to little adherent perimeters and the maximum for ρ is of course reached in circular smooth bars.

Increasing ψ and decreasing ρ traduces into an ideal improvement of the bond performances of the embedded bar.

With these positions we have that

$$\alpha = \sqrt{\frac{\kappa \Sigma}{E_1 A_1}} = \frac{1}{\sqrt{\psi \cdot \rho}} \quad (15)$$

and the dimensional function representing the ratio between yielding stresses in the core and in the bond material assumes therefore the form

$$F_{IP}(\psi, \rho) = \frac{\psi}{\sqrt{\psi \cdot \rho}} \tanh\left(\frac{L}{\sqrt{\psi \cdot \rho}}\right) \quad (16)$$

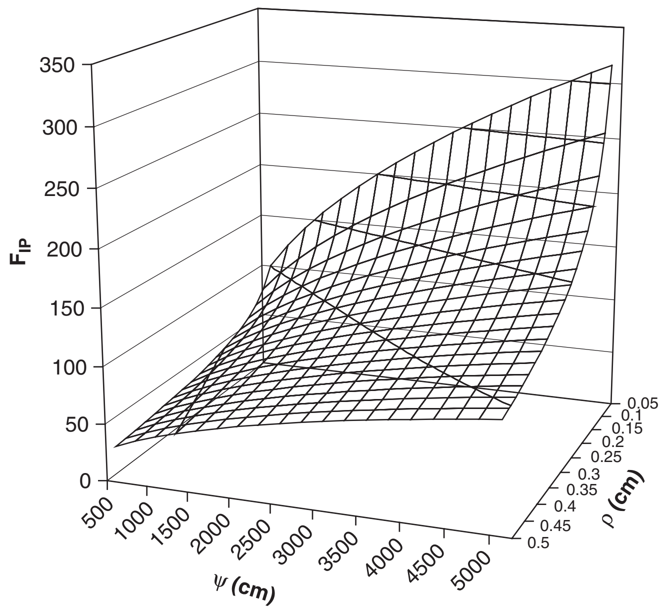

Fig. 7. Graph of the function $F_{IP} = f(\Psi, \rho)$.

which is reproduced, for a hypothetic $L = 100\,\text{cm}$, in the graph of Fig. 7.

Figs. 8 and 9 reproduce, respectively, the intersections of the surface $F(\Psi, \rho)$ with planes $\rho =$ const., and $\Psi =$ const.

From these figures it can be easily deduced how, for low values of ρ (large adherent perimeters) and increasing values of Ψ (bar material relatively stiffer than the bond material) σ_{1y} may be much higher than τ_y and still the contemporary yielding of the two materials takes place.

It can be also seen that, with large values of ρ (reduced adherent perimeters), the influence of the relative stiffness of the two materials on the satisfaction of such condition tends to vanish.

Under this limit state, anchorage length L can be deduced from Eq. (16):

$$L_{IP} = \arctan h\left[\left(\frac{\sigma_{1y}}{\tau_y}\right)\sqrt{\frac{\rho}{\psi}}\right]\sqrt{\psi\rho}. \tag{17}$$

5.2. Limit state of complete plasticity: L_{CP} anchorage length

When the outer edge E of the anchored bar initiates to yield under the force $P''_y = \sigma_{1y}A_1$ the bond material has just completed its plasticity process.

Therefore the resultant of the shear stresses is $P'''_y = L\Sigma\tau_y$.

If we impose that

$$P''_y = P'''_y, \tag{18}$$

it follows that

$$\left(\frac{\sigma_{1y}}{\tau_y}\right) = F_{CP}(\rho) = \frac{L\Sigma}{A_1} = \frac{L}{\rho} \tag{19}$$

which, in the space (F_{CP}, Ψ, ρ), is the equation of an hyperbolic cylinder parallel to the Ψ axis.

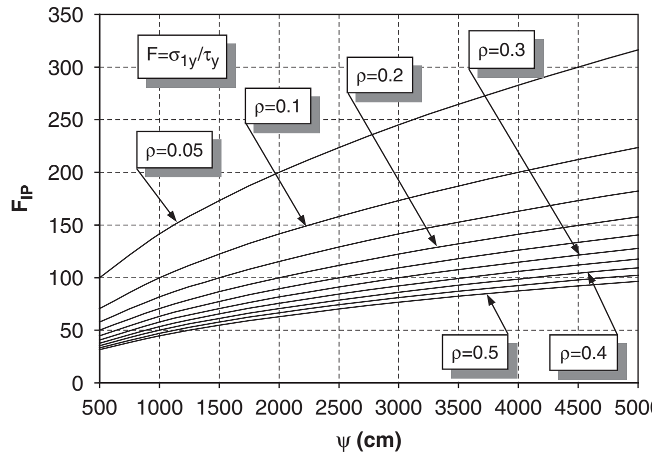

Fig. 8. Graph of the function $F_{IP} = f(\Psi, \rho = \text{const.})$.

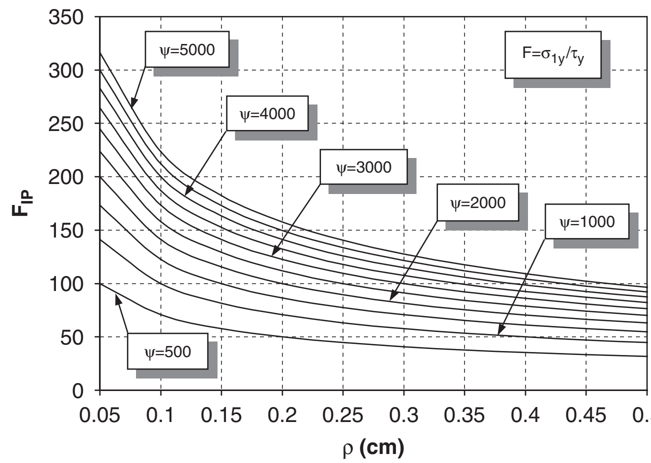

Fig. 9. Graph of the function $F_{IP} = F(\rho, \Psi = \text{const.})$.

The anchorage length is now of course independent from Ψ and linearly dependent from ρ and the ratio σ_{1y}/τ_y:

$$L_{CP} = \left(\frac{\sigma_{1y}}{\tau_y}\right)\rho. \tag{20}$$

5.3. Ratio $\Delta = L_{IP}/L_{CP}$

Let us now introduce the ratio Δ between the anchorage lengths L_{IP} and L_{CP} corresponding respectively to the yielding of the anchored bar when the bond material initiates to plasticize or is completely plasticized:

$$\Delta = \frac{L_{IP}}{L_{CP}} = \frac{\arctan h\left[(\sigma_{1y}/\tau_y)\sqrt{\rho/\psi}\right]}{(\sigma_{1y}/\tau_y)\sqrt{\rho/\psi}} > 1. \tag{21}$$

Eq. (21) is defined, for positive values of ρ and Ψ, only over the sector

$$\Psi \geqslant F^2\rho \tag{22}$$

and approaches, for any given ρ, the asymptotic value 1 if $\Psi \to \infty$.

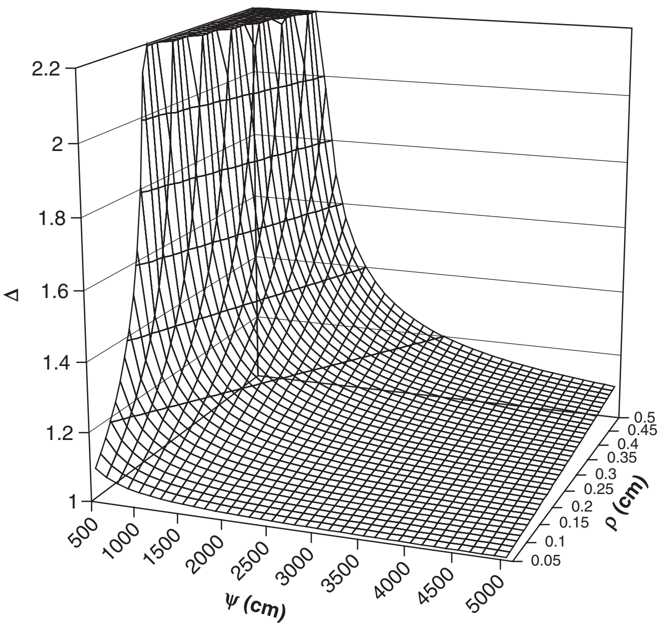

Fig. 10. 3D graph of the function $\Delta = f(\Psi, \rho)$ for $F = \sigma_{1y}/\tau_y = 50$.

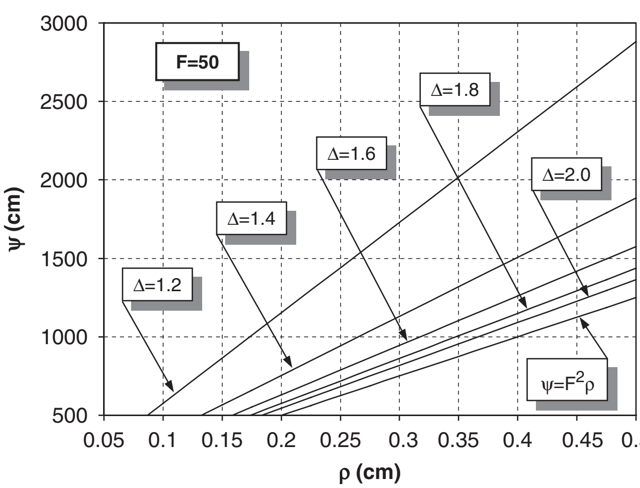

Fig. 11. Isovalues of the function $\Delta = f(\Psi, \rho)$ for $F = \sigma_{1y}/\tau_y = 50$.

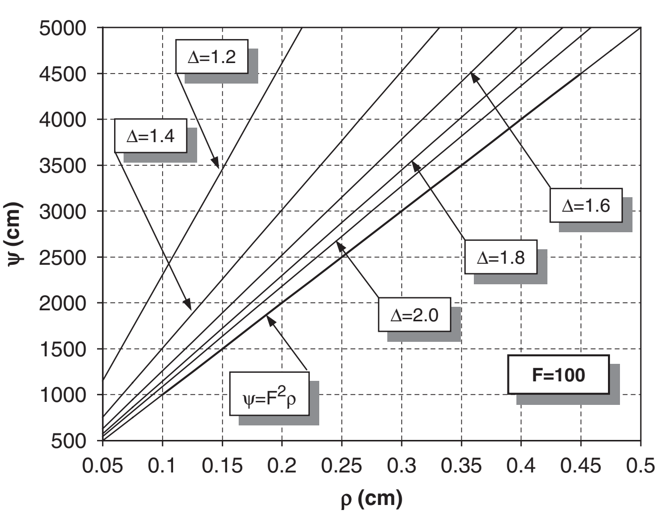

Fig. 12. Isovalues of the function $\Delta = f(\Psi, \rho)$ for $F = \sigma_{1y}/\tau_y = 100$.

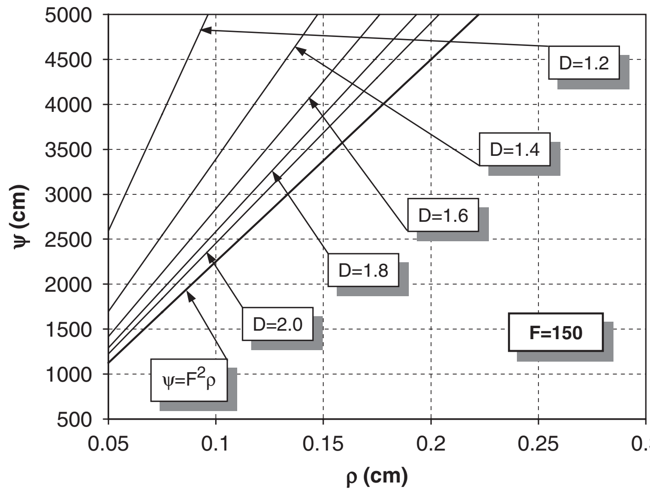

Fig. 13. Isovalues of the function $\Delta = f(\Psi, \rho)$ for $F = \sigma_{1y}/\tau_y = 150$.

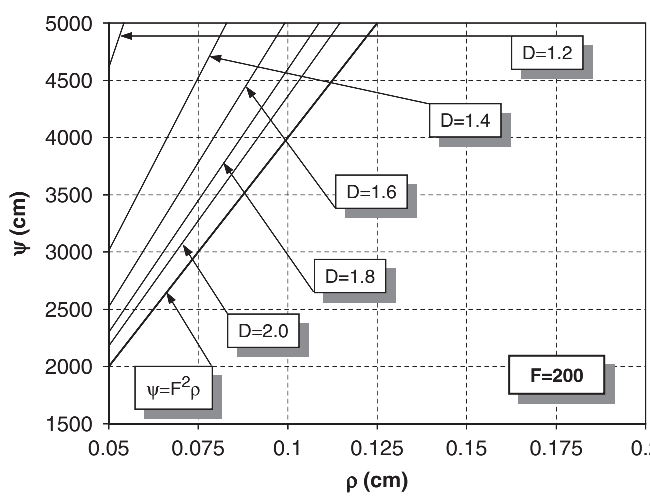

Fig. 14. Isovalues of the function $\Delta = f(\Psi, \rho)$ for $F = \sigma_{1y}/\tau_y = 200$.

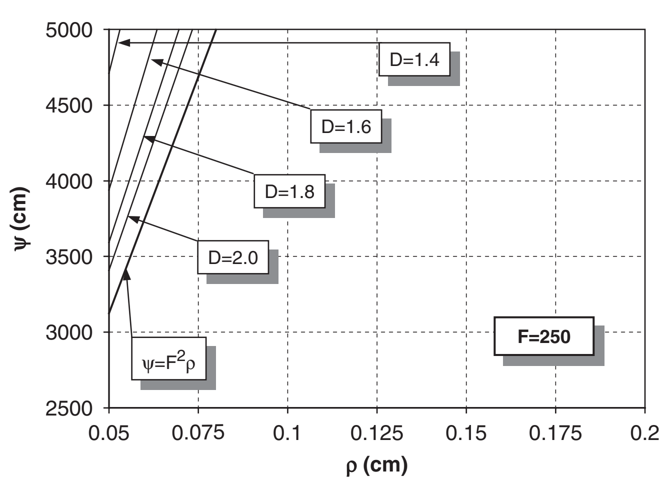

Fig. 15. Isovalues of the function $\Delta = f(\Psi, \rho)$ for $F = \sigma_{1y}/\tau_y = 250$.

In Fig. 10 is plotted, as example, the spatial distributions of $\Delta = f(\Psi, \rho)$ for $F = 50$.

Figs. 11–15 represent the distributions of the isovalues curves of $\Delta = f(\Psi, \rho)$ for different, fixed values of F.

6. Conclusions

From the preceding graphs it can be deduced that:

(1) For increasing values of the ratio $F = \sigma_{1y}/\tau_y$ between the yielding stresses of the bar and of the bond material, the definition domain of the ratio $\Delta = L_{IP}/L_{CP}$ between the anchorage lengths, respectively, at the incipient and the complete plasticization of the bond material quickly vanishes. It means that the condition of contemporary, incipient plasticity of the bar and of the bond layer can be reached only for a restricted range of the mechanical properties of the two materials (described by Ψ) and of the splice geometry (described by ρ) and also that this limit situation cannot exist if F is sufficiently great.
(2) For a given F, the ratio Δ approaches its asymptotic value 1 faster by increasing Ψ under low, constant values of ρ. That means that this ideal, unmatchable condition is better approximated in bars of large adherent perimeters.
(3) Straightforward estimation of the anchorage length L_{IP} corresponding to the simultaneously plasticity initiation in the bar and in the bond material, can be performed as shown in the following application.

7. Application

A smooth cylindrical bar of mild steel ($\phi = 2.0\,\text{cm}$, $E_1 = 21{,}00{,}000\,\text{daN/cm}^2$, $\sigma_{1y} = 2500\,\text{daN/cm}^2$) must be glued in hole previously drilled in a massive, rather rigid support.

Let us suppose that the bond material is characterized by $\tau_y = 50\,\text{daN/cm}^2$ and $k = 1400\,\text{daN/cm}^3$. We want to determine the anchorage length L_{IP}.

From $F = \sigma_{1y}/\tau_y = 50$ it follows immediately that the graph of Fig. 11 must be used.

Since $A_1 = \pi\phi^2/4 = 3.14\,\text{cm}^2$ and $\Sigma = \pi\phi$, than $\rho = \phi/4 = 0.5\,\text{cm}$ and $\Psi = E_1/k = 1500\,\text{cm}$.

From Fig. 11, for $\rho = 0.5\,\text{cm}$ and $\Psi = 1500\,\text{cm}$, we get $\Delta = L_{IP}/L_{CP} \cong 1.7$ and, since $L_{CP} = F\rho = 25\,\text{cm}$, we finally obtain $L_{IP} = 42.5\,\text{cm}$.

Let us now suppose to use a bar of equivalent square cross section (size $l = 1.773\,\text{cm}$).

F and Ψ remain unchanged while $\rho = 0.44\,\text{cm}$ because the adherent perimeter is now nominally grown up to $\Sigma = 41 = 7.09\,\text{cm}$.

From Fig. 11, for $\rho = 0.44\,\text{cm}$ and $\Psi = 1500\,\text{cm}$, we get $\Delta = L_{IP}/L_{CP} \cong 1.55$ and, since $L_{CP} = F\rho = 22\,\text{cm}$, we obtain $L_{IP} = 1.55 \times 22 = 34.1\,\text{cm}$.

Therefore, with an increase of the adherent perimeter of about 13% the anchorage length L_{IP} decreases of about 20%.

References

[1] Zamora NA, Cook RA, Konz RC, Consolazio G. Behavior and design of single, headed and unheaded grouted anchors under tensile load. ACI Structural Journal 2003;100(2):222–30.

[2] L'Hermite R, Bresson J. Béton armé d'armatures collées, Colloque Rilem: Recherches Expérimentales sur les nouveaux développements apportés par les résines synthétiques aux techniques de construction, U.T.I., vol. II, Paris, France, 1967. p. 1–55 [in French].

[3] CEB Bulletin d'Information No. 151. Bond action and bond behaviour of reinforcement. State of the art report. Paris, France: Comité Euro—International du Béton; 1982. p. 153.

[4] CEB Bulletin d'Information No. 181. Anchorage zones of prestressed concrete members. State of the art Report. Lausanne, Switzerland: Comité Euro—International du Béton; 1987. p. 137.

[5] ACI Committee 408. State of the art Report on bond under cyclic loads. Farmington Hills, Michigan, USA: American Concrete Institute ACI 408.2R-92; 1992.

[6] FIB Bulletin No. 10. Bond of reinforcement in concrete. State-of-art-report. Féderation International du Béton, 153, Stuttgart, Germany, 2000.

[7] Losberg A. Anchorage of beam reinforcement shortened according to the moment distribution curve, seventh congress IABSE, Final Report, Rio de Janeiro, Brazil, 1964. p. 383–92.

[8] Tepfers R. A theory of bond applied to overlapped tensile reinforcement splices for deformed bars, Pubbl. 73/2, Division of Concrete Structures, Chalmers University of Technology, 328, Göteborg, Sweden, 1973.

[9] Bleich F. Theorie und Berechnung der eisernen Brücken. Germany, Berlin: Springer; 1924. p. 306–14 [in German].

[10] Tassios TP, Yannapoulos PJ. Analytical studies on reinforced concrete members under cyclic loading based on bond stress–slip relationships. ACI Journal 1981;78(3):206–16.

[11] Ciampi V, Eligehausen R, Bertero VV, Popov EP. Analytical model for concrete anchorages of reinforcing bars under generalised excitations, Report no. UCB/EERC 82–83, University of California at Berkeley, California, 1982.

[12] Filippou FC, Popov EP, Bertero VV. Modeling of reinforced concrete joints under cyclic exitations. ASCE, Journal of Structural Engineering 1983;109(11):2666–84.

[13] Russo G, Zingone G, Romano F. Analytical solution for bond–slip of reinforcing bars in r.c. joints. ASCE Journal of Structural Engineering 1990;116(2):336–55.

[14] Ivanyi M, Baniotopoulos CC. Semi-rigid connections in structural steelwork. Udine, Italy: C.I.S.M.; 2000.